Radiation Characteristics of a Conical Helix of Low Pitch Angle

J. S. Chatterjee

Citation: Journal of Applied Physics **26**, 331 (1955); doi: 10.1063/1.1721988
View online: http://dx.doi.org/10.1063/1.1721988
View Table of Contents: http://scitation.aip.org/content/aip/journal/jap/26/3?ver=pdfcov
Published by the AIP Publishing

Radiation Characteristics of a Conical Helix of Low Pitch Angle

J. S. CHATTERJEE
Institute of Radio Physics and Electronics, Calcutta University, Calcutta, India
(Received August 10, 1953)

The present work is an extension of the author's prior work on the radiation characteristics of and current distribution in a conical helix, the helix used in the present case having a pitch angle much lower than of that studied previously. In this case the condition of the phase velocity adjusting itself automatically to maintain maximum directivity condition (which enables the radiation to be confined in the axial mode over a large band of frequencies) does not hold. Nevertheless the major fraction of energy could be radiated in the axial direction when the geometry of the helix and the distance of the apex from the ground were properly chosen, the conical helix together with the ground being regarded as tapered transmission lines (with the ground as one and the helix wire—with the distance of its elements from the ground line increasing continually,—as the other line).

Measurements of the field intensity and the current distribution were made in the frequency range of 100 Mc/sec to 500 Mc/sec with a conical helix antenna arrangement as follows. The helix was of six turns, the radius increasing uniformly from 5 cm at the apex to 65 cm at the base within an axial distance of 60 cm. The apex of the helix was placed at a distance of 17.5 cm from the "ground" provided by a 6-ft square copper netting of close mesh. It was found that within the range of frequency measured the major fraction of the energy was radiated in the axial direction. Theoretical expressions for E_ϕ and E_θ were derived by assuming a linear current distribution, and the calculated radiation patterns were found to agree with the experimentally determined ones.

I. INTRODUCTION

A CYLINDRICAL helix is known to act as an efficient antenna when the length of one turn of the helix is comparable with the wavelength. Depending upon the ratio of the diameter to wavelength and pitch angle, the helix can radiate in three different modes. When the helix is conical, instead of cylindrical, its radiation characteristics change markedly. This has been studied[1] by the author for the case of a conical helix with pitch angle of 6°. It was found that when the base was near the ground and the feed was at the apex, the axial mode of radiation could be maintained over a band width much greater than one octave. Further, depending upon the limitations imposed by the practical difficulty of obtaining the smallest radius at the apex of the helix the band width can be increased to any desired extent.

In both the cylindrical and conical helices studied the maintenance of the axial mode of radiation over a large band width is due to the fact that the phase velocity along the helical conductor so adjusts itself automatically, that the condition of maximum directivity along the axis holds.[2] Further, in all these antennas, the "ground" plane is provided by a small conducting sheet placed very close to the helix, the "ground" serving as a launching device rather than as an image plane.

In this present paper we will describe the results of investigations on the radiation characteristics of a conical helix with pitch angle much lower than that studied above. The pitch angle, in fact, is so low that the condition of automatic adjustment of phase velocity does not hold. Further, the "ground" plane is made sufficiently large to allow the image to be well formed. Under such conditions the helix, mounted with its apex at a small appropriate distance above the "ground" plane, was found to radiate in the axial direction over a frequency range 5:1, which is much higher than the range for the conical helix previously considered.

In the next section will be described the results of experiments made on the determination of the polar diagram and the charge distribution along the length of such a conical helix of low pitch angle. Analysis for theoretical determination of the radiation pattern will then follow.

2. EXPERIMENTS WITH THE CONICAL HELIX

The conical helix used had the following dimensions. It was made of $\frac{5}{32}$-in. brass rod and had 6 turns. The radius at the apex was 5 cm and increased uniformly to 65 cm at the base within a height of 60 cm. A copper wire netting (40 per in., 6 ft square) provided the "ground." The apex of the helix was at a distance of 17.5 cm from the ground plane. It was excited by a

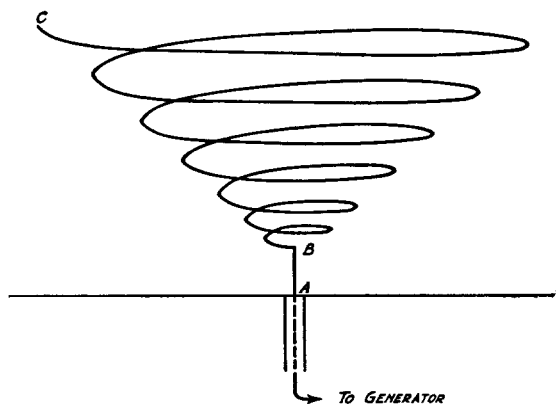

FIG. 1. Illustrating the method of feeding energy to the conical helix with respect to "ground."

[1] J. S. Chatterjee, J. Appl. Phys. **24**, 550 (1953).
[2] J. D. Kraus. Proc. Inst. Radio Engrs. **37**, 263 (1949).

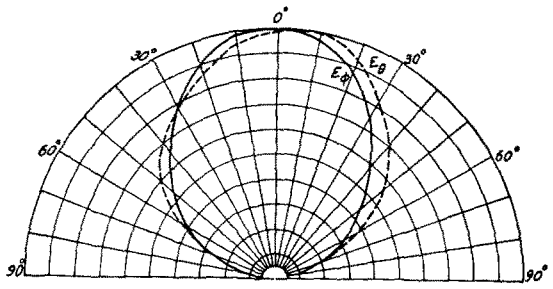

(a)

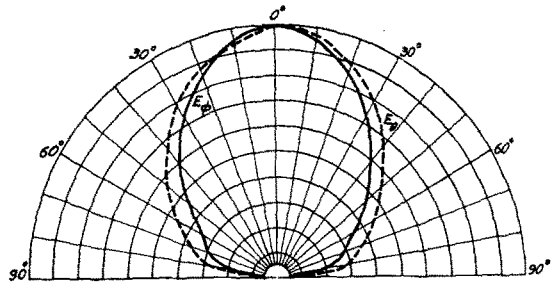

(b)

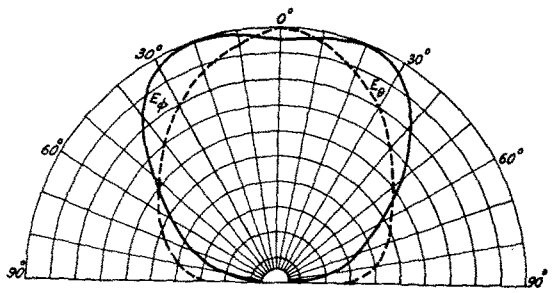

(c)

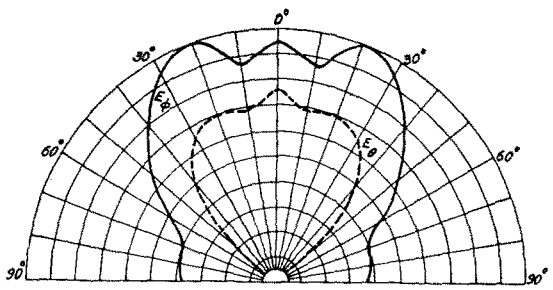

(d)

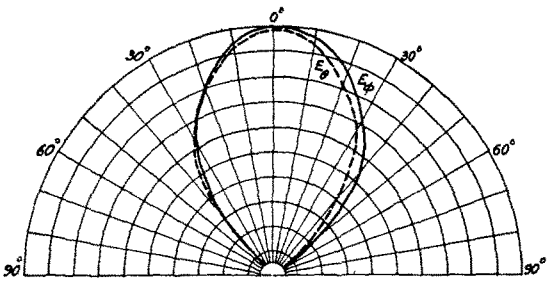

(e)

co-axial feeder, the outer conductor of which was connected to the ground plane and the inner to the apex as shown in Fig. 1. For the purpose of field measurements the helix system was mounted 12 ft above the floor level with the axis horizontal.

Measurement of Electric Field

The vertical and horizontal components of the electric field were measured with a small dipole placed at a distant point and at the same height as the axis of the helical antenna. The polar diagrams obtained for a number of frequencies in the range 100 Mc to 500 Mc are shown in Fig. 2. The frequencies were fairly closely spaced and it was unlikely that the radiation patterns deteriorated in any of the intermediate frequencies. This is because the radiation patterns were not found to change markedly in form from one frequency to the next.

Measurement of Charge Distribution

The charge distribution was measured by coupling capacitively a small probe to different parts of the helix conductor. The charge distribution for a number of frequencies in the range 100 Mc–500 Mc are shown in Figs. 3 and 4. The polar diagrams show that over a large range of frequencies the major fraction of the energy is radiated in the axial direction.

The following points may be noted from the charge distribution curves.

(a) The current is gradually attenuated along the helix and, for frequencies higher than 220 Mc, the current is completely attenuated at the end becoming entirely progressive. The charge and current distributions in this case are identical.

(b) For frequencies lower than 220 Mc, the current is not completely attenuated at the end and hence there is reflection. There are thus standing waves at the end of the helix due to which polar diagrams may be expected to be different from the case when only progressive current exists. If, however the reflected wave is not strong, its effect at the input end is negligible since it is further attenuated as it travels backwards.

(c) It follows from (a) that the helix presents a constant impedance at the input for all frequencies higher than 220 Mc.

3. THEORETICAL ANALYSIS

We shall derive expressions for the radiation field in the θ plane for the case when only progressive current is present. The radiation field for the general case can

FIG. 2. (a) E_ϕ and E_θ radiation patterns of the conical helix shown in Fig. 1. Frequency, 100 Mc/sec. (b) E_ϕ and E_θ radiation pattern of the conical helix shown in Fig. 1. Frequency, 220 Mc/sec. (c) E_ϕ and E_θ radiation pattern of the conical helix shown in Fig. 1. Frequency, 300 Mc/sec. (d) E_ϕ and E_θ radiation pattern of the conical helix in Fig. 1. Frequency, 400 Mc/sec. (e) E_ϕ and E_θ radiation patterns of the conical helix shown in Fig. 1. Frequency, 500 Mc/sec.

be obtained by adding the field produced by the reflected wave in correct phase.

The field at a distant point consists of the following components: (a) field of the helix BC (Fig. 1), (b) field of the image of the helix, (c) field of the length AB (Fig. 1), and (d) field of the image of (c).

We will calculate the fields separately for each of the above components and add them vectorially to get the total radiation field.

The electric field[3] at the distant point is given by

$$E=\frac{j\omega\mu_0}{4\pi R}\int[\mathbf{r}_0\times(\mathbf{r}_0\times\mathbf{s}_0)]Ie^{-j\beta R}ds, \qquad (1)$$

where ω = angular frequency, μ_0 = the absolute permeability of space, ds = an element of the helix conductor carrying a current I, R = distance from the elements ds of the point at which electric field is to be calculated, $\mathbf{r}_0$ = the unit radial vector in a spherical co-ordinate system (r,θ,ϕ) with the helix at the origin,

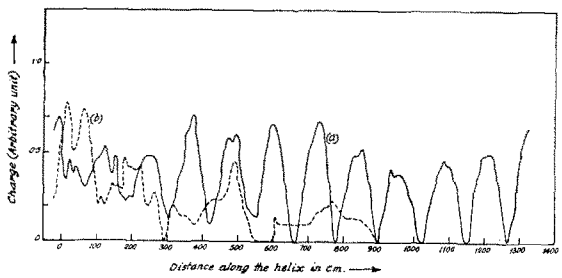

FIG. 3. Charge distribution along the length of the conical helix shown in Fig. 1. The zero point of the abscissa is at B. Excitation frequency, (a) 100 Mc/sec, (b) 220 Mc/sec.

and $\mathbf{s}_0$ = the unit vector along the axis of the helix conductor.

To calculate the field of the helix we first calculate the field for one of the turns and then combine the fields of all the turns. This is possible if the phase velocity along the helix is known.

The equation of the form of a simple conical helix in cylindrical coordinates is given by

$$a=a_0(1+k\phi), \qquad (2)$$

where a = the distance of an element from the axis. Also

$$dz=a\tan\alpha d\phi, \qquad (3)$$

or

$$z=\int_0^{\phi}a_0(1+k\phi)\tan\alpha d\phi$$

$$=a_0\tan\alpha(1+\tfrac{1}{2}k\phi)\phi, \qquad (4)$$

where α = the inclination of an element of the antenna with the horizontal plane and is constant. From the

[3] R. W. P. King, *Electromagnetic Engineering* (McGraw-Hill Book Company, Inc., New York, 1945), Vol. I, p. 271.

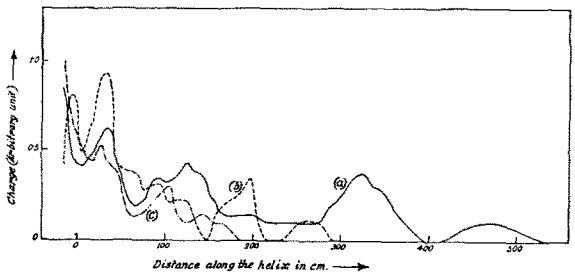

FIG. 4. Charge distribution along the length of the conical helix shown in Fig. 1. The zero point of the abscissa is at B. Excitation frequency, (a) 300 Mc/sec, (b) 400 Mc/sec, (c) 500 Mc/sec.

helix geometry it follows that for the mth turns,

$$ds=a_m(1+k_m\phi), \qquad (5)$$

$$s=a_m\sec\alpha(1+\tfrac{1}{2}k_m\phi)\phi, \qquad (6)$$

where s = length of helix conductor from 0 to ϕ. The distance of an element ds in the mth turn from the distant point is given by (Fig. 5) where z_m and a_m are the values of z and a at $\phi=0$ in the mth turn, and k_m is the value of k when the equation of the helix is written such that $\phi=0$ at the center of mth turn.

$$R_m=R_0-(z_m+z)\cos\theta-a\sin\theta\cos\phi$$
$$=R_0-z_m\cos\theta-a_m\tan\alpha\phi(1+\tfrac{1}{2}k_m\phi)\cos\theta$$
$$-a_m(1+k_m\phi)\sin\theta\cos\phi, \qquad (7)$$

The current falls off exponentially along the helical conductor. For simplicity of calculation it is, however, assumed that the current is constant over a turn and then changes by appropriate amount in the next adjacent turn. Thus, the current in the mth turn is given by

$$I=I_m'e^{-j\nu_m}e^{-j\beta s}, \qquad (8)$$

where I_m' is the value of current at $\phi=0$ in the mth turn and ν_m is the phase difference between the center of mth turn and current at the input.

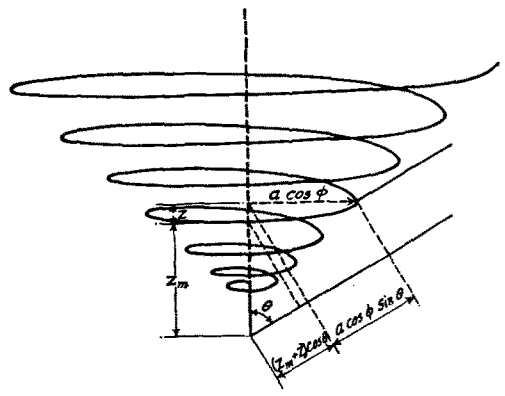

FIG. 5. Illustrating the calculation of the distance from a point in the far zone, of an element ds of a loop of the helix with reference to the distance of the same point from the origin.

Substituting Eqs. (8) and (5) in Eq. (1),

$$E_m=\frac{j\omega\mu_0}{4\pi R_0}\int[-\boldsymbol{\phi}s_\phi-\boldsymbol{\theta}s_\theta]I_m'e^{-j\nu_m}e^{-j\beta R_m}\times a_m(1+k_m\phi)\sec\alpha]d\phi. \quad (9)$$

In this equation we have replaced R_m by R_0, except in the phase term. The direction cosines between $\mathbf{s}_0$ and the ϕ, θ, spherical coordinate axes are given by

$$S_\phi=\cos\alpha\left[\cos\phi+\frac{k_m\sin\phi}{1+k_m\phi}\right], \quad (10)$$

$$S_\theta=-\cos\alpha\cos\theta\left[\sin\phi-\frac{k_m\cos\phi}{1+k_m\phi}\right]-\sin\alpha\sin\theta. \quad (11)$$

Substituting Eqs. (7) and (10) in Eq. (9) and rearranging terms, the component of the electric field at the distant point for the mth turn is given by

$$E_\phi{}^m=-\frac{j\omega\mu_0e^{-j\beta R_0}}{4\pi R_0}a_mI_me^{-j\nu_m}e^{j\beta z_m\cos\theta}\times\int_{-\pi}^{+\pi}\Big[\{\cos\phi(1+k_m\phi)+k_m\sin\phi\}\times\exp-j(\beta a_m\sec\alpha-\beta a_m\tan\alpha\cos\theta)\phi\times\exp-j\left(\beta a_m\sec\alpha\frac{k_m}{2}-\beta\alpha_m\frac{k_m}{2}\tan\alpha\cos\theta\right)\phi^2\times\exp(\delta j\beta a_m\sin\theta\cos\phi)\times\exp(j\beta a_mk_m\sin\theta\phi\cos\phi)\Big]d\phi. \quad (12)$$

We introduce the following abbreviations,

$$E_0=\frac{j\omega\mu_0I_0\exp(-j\beta R_0)}{4\pi R_0},$$

$$g_m=\beta a_m\sec\alpha,$$

$$b_{\theta m}=\beta a_m\tan\alpha\cos\theta,$$

$$D'=\beta a_m\sec\alpha\frac{k_m}{2}-\tfrac{1}{2}a_mk_m\beta\tan\alpha\cos\theta=D-\delta,$$

$$p_{\theta m}=\beta a_mk_m\sin\theta,$$

$$d_{\theta m}=\beta a_m\sin\theta,$$

$$\eta_{\theta m}=\beta z_m\cos\theta,$$

$$I_m'/I_0=I_m. \quad (13)$$

Since D' is small and $\phi^2\leqq\pi^2$, we put

$$\exp(-jD'\phi^2)\fallingdotseq(1-jD'\phi^2). \quad (14)$$

Further, since $p_{\theta m}$ is very small except near $\theta=\pi/2$ and $\phi=\pi$, we put

$$\exp(jp_{\theta m}\phi\cos\phi)\fallingdotseq 1. \quad (15)$$

We also note that

$$\exp(jd_{\theta m}\cos\phi)\sum_{-\infty}^{+\infty}\gamma^nJ_n(d_{\theta m})\exp(jn\phi, \quad (16)$$

where $J_n(d_{\theta m})$ is the nth root of the Bessel function for the argument $d_{\theta m}$.

Using (14), (15), and (16), and neglecting $k_mD'\phi^2$ and $k_mD'\phi^3$, the field $E_{\phi h}$ due to helix alone is obtained by carrying out the integration in Eq. (12) and is given by

$$E_{\phi h}=-E_0\sum_{m=1}^{N}a_mI_me^{-j\nu_m}e^{j\eta_{\theta m}}\sum_{-\infty}^{+\infty}j^nJ_n(d_{\theta m})\times\Big[\Big\{(1-jk_m)\frac{\sin x\pi}{x}+k_m\left(-j\pi\frac{\cos x\pi}{x}+j\frac{\sin x\pi}{x^2}\right)-jD'\left(\pi^2\frac{\sin x\pi}{x}+\frac{2\pi\cos x\pi}{x^2}-\frac{2\sin x\pi}{x^3}\right)\Big\}+\Big\{(1+jk_m)\frac{\sin y\pi}{y}+k_m\left(-j\pi\frac{\cos y\pi}{y}+j\frac{\sin y\pi}{y^2}\right)-jD'\left(\pi^2\frac{\sin y\pi}{y}+2\pi\frac{\cos y\pi}{y^2}-\frac{2\sin y\pi}{y^3}\right)\Big\}\Big], \quad (17)$$

where

$$x=n-g_m+b_{\theta m}+1=\nu+1,$$
$$y=n-g_m+b_{\theta m}-1=\nu-1. \quad (18)$$

Putting

$$j\pi\frac{\cos x\pi}{x}+j\frac{\sin x\pi}{x}=f_x, \quad (19)$$

$$\pi^2\frac{\sin x\pi}{x}+2\pi\frac{\cos x\pi}{x^2}-\frac{2\sin x\pi}{x^3}=F_x, \quad (20)$$

the total field due to the real source and image is given by

$$E_\phi=E_0\sum_{m=1}^{N}a_mI_m\exp(-j\nu_m)\sum_{-\infty}^{+\infty}j^nJ_n(d_{\theta m})\times\Big[\Big\{(1-jk_m)\left(\frac{\sin x'\pi}{x'}e^{-j\eta_{\theta m}}-\frac{\sin x\pi}{x}e^{j\eta_{\theta m}}\right)+(1+jk_m)\left(\frac{\sin y'\pi}{y'}e^{-j\eta_{\theta m}}-\frac{\sin y\pi}{y}e^{j\eta_{\theta m}}\right)+k_m\{(f_{x'}+f_{y'})e^{-j\eta_{\theta m}}-(f_x+f_y)e^{j\eta_{\theta m}}\}-jD\{(F_{x'}+F_{y'})e^{-j\eta_{\theta m}}-(F_x+F_y)e^{j\eta_{\theta m}}\}\Big], \quad (21)$$

where

$$x'=n-b_{\theta m}-g_m+1=\nu'+1,$$

$$y'=n-b_{\theta m}-g_m-1=\nu'-1.$$

In Eq. (21) we have neglected δ.

To calculate the θ component of the electric field we note that E_θ is given by

$$E_\theta=E_{\theta h}+E_{\theta h}'+(E_{\theta A}+E_{\theta A}'), \tag{22}$$

where $E_{\theta h}$=field produced by the helix, $E_{\theta h}'$=field produced by the image of the helix, and $E_{\theta A}$ and $E_{\theta A}'$ are fields caused by the axial length of the antenna and its image, respectively.

We note that

$$E_{\theta A}+E_{\theta A}'=-2E_0lj\sin\theta\frac{1-\cos\beta l(1-\cos\theta)}{\beta l(1-\cos\theta)}, \tag{23}$$

where l, the length AB (Fig. 1) carries a uniform current I_0.

Proceeding as before we obtain from Eq. (22) the θ component of the electric field E_θ, which is given by

$$\begin{aligned}E_\theta=E_0\sum_{m=1}^{N}a_mI_m\exp(-j\nu_m)\sum_{-\infty}^{+\infty}j^nJ_n(d_{\theta m})\\
\times\Bigg[\cos\theta\Bigg\{(-j-k_m)\left(\frac{\sin x'\pi}{x'}e^{-i\eta_{\theta m}}-\frac{\sin x\pi}{x}e^{i\eta_{\theta m}}\right)\\
\times(-j+k_m)\left(\frac{\sin y'\pi}{y'}e^{-i\eta_{\theta m}}-\frac{\sin y\pi}{y}e^{i\eta_{\theta m}}\right)\Bigg\}\\
-k_m\cos\theta\{(f_{x'}-f_{y'})e^{-i\eta_{\theta m}}-(f_x-f_y)e^{i\eta_{\theta m}}\}\\
+D\cos\theta\{(F_{x'}-F_{y'})e^{-i\eta_{\theta m}}-(F_x-F_y)e^{i\eta_{\theta m}}\}\\
+2\sin\theta\tan\alpha\Bigg\{\left(\frac{\sin\nu'\pi}{\nu'}e^{-i\eta_{\theta m}}-\frac{\sin\nu\pi}{\nu}e^{i\eta_{\theta m}}\right)\\
+jk_m(f_{\nu'}e^{-i\eta_{\theta m}}-f_\nu e^{i\eta_{\theta m}})-jD(F_{\nu'}e^{-i\eta_{\theta m}}+F_\nu e^{i\eta_{\theta m}})\Bigg\}\\
-2E_0lj\sin\theta\frac{1-\cos\beta l(1-\cos\theta)}{\beta l(1-\cos\theta)}\Bigg].\end{aligned} \tag{24}$$

4. DISCUSSION

The E_ϕ and E_θ components of the electric field at the distant point may be computed from the right-hand expressions of Eqs. (21) and (24), respectively. The expressions are long and complicated but fortunately, for practical computation, a number of approximating assumptions may be made since some of the terms are quite small compared to others. For example, the terms involving $\tan\alpha$ may be neglected as $\tan\alpha=0.045$. Again, in most of the cases only the terms $J_0(d_{\theta m})$ and $J_{\pm1}(d_{\theta m})$ in the summation $\sum_{-\infty}^{+\infty}j^nJ_n(d_{\theta m})$ need be retained. The higher order term $J_2(d_{\theta m})$ needs consideration only for the fields due to bigger turns and for large angles. Also, $\sum_{m=1}^{N}a_mI_m$ need not be considered for all the turns, as its contribution is significant only for the turns in which the current has not died out completely. Thus, in the case of 300 Mc, only 4 turns are to be considered, because the current in the fifth turn is zero. The computed values of E_ϕ and E_θ from Eqs. (21) and (24) for 300 Mc are plotted in Fig. 6 for comparison with the experimentally obtained curves. Only first-order terms have been retained in the computation.

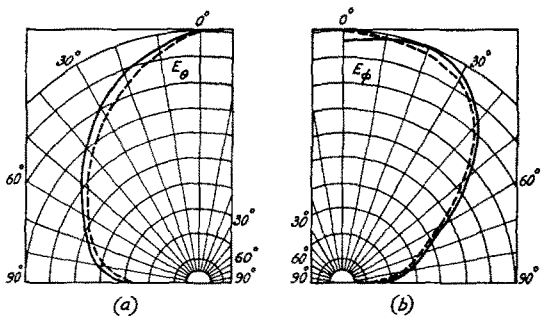

FIG. 6. Calculated (dotted lines) and experimentally observed (solid lines) radiation patterns of (a) E_θ and (b) E_ϕ. Frequency, 300 Mc/sec.

An examination of the curves in Fig. 2 shows that over a large band of frequencies the radiation pattern from the conical helix with low pitch angle is a single lobe with the maximum in the axial direction. This effect is similar to that already considered for a conical helix with moderate pitch angle, though as already pointed out, the condition of phase velocity adjustment, necessary for maximum directivity condition does not hold in this case. That a major fraction of energy is still radiated in the axial direction is due to the fact that the geometry of the helix and the distance of the apex from the ground have been chosen appropriately. The conical helix together with the ground in this case may be regarded as tapered transmission lines. The ground is one of the "lines" and the helix wire, with the distance of its elements from the ground continually increasing, is the other "line."

Regarding the property of maintenance of axial mode of radiation over a large band of frequencies, there is little to choose between the two types of conical helices (moderate or low pitch angle). For radiation in the vertical direction, the latter, however, on account of its smaller axial height for the number of turns required, possesses a greater practical advantage over the former where the helix is to be designed for low frequencies. This is because for such frequencies helices of moderate pitch angle become unmanageably large.

ACKNOWLEDGMENT

Grateful thanks are due Professor S. K. Mitra for constant encouragement and many helpful discussions during preparation of the paper.